BioRisk 18: 115–132 (2022)
doi: 10.3897/biorisk.18.86616
https://biorisk.pensoft.net

RESEARCH ARTICLE

A peer-reviewed open-access journal
BioRisk

Potential risk resulting from the influence of static magnetic field upon living organisms. Numerically simulated effects of the static magnetic field upon metalloporphyrines

Wojciech Ciesielski[1], Tomasz Girek[1], Zdzisław Oszczęda[2], Jacek A. Soroka[3], Piotr Tomasik[2]

1 *Institute of Chemistry, Jan Długosz University, 42 201 Częstochowa, Poland* **2** *Nantes Nanotechnological Systems, 59 700 Bolesławiec, Poland* **3** *Scientific Society of Szczecin, 71-481 Szczecin, Poland*

Corresponding author: Wojciech Ciesielski (w.ciesielski@interia.pl)

Academic editor: Josef Settele | Received 16 May 2022 | Accepted 31 July 2022 | Published 23 August 2022

Citation: Ciesielski W, Girek T, Oszczęda Z, Soroka JA, Tomasik P (2022) Potential risk resulting from the influence of static magnetic field upon living organisms. Numerically simulated effects of the static magnetic field upon metalloporphyrines. BioRisk 18: 115–132. https://doi.org/10.3897/biorisk.18.86616

Abstract

Background: An attempt to recognize the effects of a static magnetic field (SMF) of varying flux density on flora and fauna.. For this purpose the influence of static magnetic field upon molecules of Mg(II), Fe(II), Fe(III), Co(II), Co(III) and Cu(II) metalloporphyrins is studied.

Methods: Computations of the effect of real SMF 0.0, 0.1, 1, 10 and 100 AFU (Arbitrary Magnetic Field Unit; here 1AMFU > 1000 T) flux density were performed in silico (computer vacuum) involving advanced computational methods.

Results: The static magnetic field (SMF) decreased the stability of the metalloporphyrine molecules. This effect depended on the situation of the molecule in respect to the direction of the SMF of the Cartesian system. An increase in the value of heat of formation was accompanied by an increase in the dipole moment. It was an effect of deformations of the molecule which involved pyrrole rings holding the hydrogen atoms at the ring nitrogen atoms and the length of the C-H and N-H bonds. As a consequence, that macrocyclic ring lost its planarity.

Conclusions: SMF even of the lowest, 0.1 AMFU flux density influences the biological role of metalloporphyrines associated with their central metal atoms. This effect is generated by changes in the electron density at these atoms, its steric hindering and polarization of particular bonds from pure valence bonds possibly into ionic bonds.

Keywords
Co(II)porphyrine, Co(III)porphyrine, Cu(II)porphyrine, Fe(II)porphyrine, Fe(III)porphyrine, Mg(II) porphyrine

Introduction

Our previous paper (Ciesielski et al. 2022) described the effect of Static Magnetic Field (SMF) of 0.1 to 100 AMFU (Arbitrary Magnetic Field Unit. 1 AMFU > 1000 T) upon porphine. Porphine and its derivatives are precursors of several biologically important compounds. They are derivatives of protoporphyrine IX. (Kadish et al. 2000; Ortiz de Montellano 2008). A biological activity of porphine results from two ways of its modification. One of them is binding various functional groups as external substituents of protoporphyrin IX. For instance, in such a way proteins like cysteine which are bound via thioether bonds form *C*-type cytochromes essential for the life of virtually all organisms (Stevens et al. 2004). The second way of modification involves coordination of metal ions inside the porphine ring to form metalloporphyrines. One of the most common representatives of metalloporphyrines are chlorophylls containing Mg atom inside the porphine ring. In chlorophylls, its presence is responsible for the green color of those compounds. Chlorophyll is a group of 6 compounds which differ from one another with substituents of the macrocyclic ring. Two of them (chlorophylls *a* and *b*) exist in the photosystem (chloroplasts) of green plants and algae. They absorb sunlight, employing its energy to synthesize carbohydrates from CO_2 and water. It is so-called photosynthesis. Several green chlorophyll pigments reside also in mesosomes of cyanobacteria. Animals and humans obtain chlorophyll as the component of their diet. During photosynthesis, plants take in carbon dioxide (CO_2) and water (H_2O) from the air and soil. Within the plant cell, the water is oxidized, meaning it loses electrons, while the carbon dioxide is reduced, meaning it gains electrons. This transforms the water into oxygen and the carbon dioxide into glucose. Magnesium in chlorophylls provides absorption of the blue and red potion of the electromagnetic spectrum, leaving the green portion of that spectrum non-absorbed. It does not constitute any particular reaction site for water and carbon dioxide (Kadish et al. 2000; Ortiz de Montellano 2008).

In metalloporphyrines holding either Fe(II), Fe(III), Co(II), Co(III) or Cu(II) these central atoms of the complexes act as coordination sites. Porphine derivatives with Fe(II) and Fe(III) ions coordinated and chemically bound within the macrocyclic ring are called hem and hemin, respectively. They are red-coloured compounds constituting the animal and human blood. Ferrous cation in heme can coordinate such as molecular oxygen, carbon monoxide, cyanide anion and other ligands. In hemin Fe(III) atom utilizes one of its valence bonds for binding chlorine atom. It is formed from a hem group, such as hem B found in the hemoglobin of human blood (Kadish et al. 2000; Ortiz de Montellano 2008).

Porphine derivatives coordinated to the Co(II) and Co(III) ions are known as vitamin B_{12}, (cobalamin). It is a cofactor in DNA synthesis, in both fatty acid and amino

acid metabolism. It is essential for the normal functioning of the nervous system and the maturation of red blood cells in the bone marrow (Kadish et al. 2000; Ortiz de Montellano 2008).

In the organisms of some invertebrates such as snails, lobsters and spiders, oxygen is transported by hemicyanines containing Cu(II) atom instead of Fe(II)/Fe(III) ions. Such hemocyanines (hemolymph) carrying coordinated oxygen are blue colored. Hence these invertebrates have blue blood (Walter et al. 2010).

Recently, numerous synthetic derivatives of the parent porphine in the form of metalloporhyrines have found their application in the material sciences of engineering, chemistry, physics, biology, and medicine (Anderson et al. 1995; Kadish et al. 2000; Yella et al. 2011; Ptaszek 2013 Huang et al. 2015), particularly in anticancer photodynamic therapy (Hodak and Pavlovsky 2015).

The subject of this paper focuses on the effect of SMF of 0.1 to 100 AMFU (Arbitrary Magnetic Field Unit) upon Mg (II), Fe(II), Fe(III), Co(II), Co(III), and Cu(II) porphyrines as the most essential and most common in functioning organisms of flora and fauna. The target is achieved involving in silico (computer vacuum) advanced computational methods.

Numerical computations

DFT (Density Functional Theory) Molecular structures were drawn using the Fujitsu Scigress 2.0 software (Marchand et al. 2014). Their principal symmetry axes were oriented along the x, y and z-axes of the Cartesian system. The magnetic field was fixed in the same direction, with the south pole from the left side.

Z axis is perpendicular to the porphine plane, the x and y axes are in the plane of the system, each of them along two nitrogen atoms. Because of mesomerism only, due to quaternary symmetry z axis the last two axes are undistinguished and symmetry D_{4h} is observed (Scheidt and Lee 1987). Since pairs of the nitrogen atoms differ from one another, the x axis cross two nitrogen atoms substituted by hydrogen atoms and y axis cross remains two unsubstituted nitrogen atoms and itself both axis x,y are distinguished.

Subsequently, involving Gaussian 0.9 software equipped with the 6–31G** basis (Frisch et al. 2016), the molecules were optimized and all values of bond length, dipole moment, total energy, heath of formation, bond energy and HOMO/LUMO energy level for single molecules.

In the consecutive step, influence of static magnetic field (SMF) upon optimized molecules were computed with Amsterdam Modelling Suite software (Farberovich and Mazalova 2016; Charistos and Munoz-Castro 2019) and the NR_LDOTB (nonrelativistic orbital momentum L-dot-B) method (Glendening et al. 1987; Carpenter and Weinhold 1988). Following that step, using Gaussian 0.9 software equipped with the DFT with functional B3LYP 6–31G** basis (Charistos and Munoz-Castro 2019) values of bond length, dipole moment, heath of formation equal to the energy

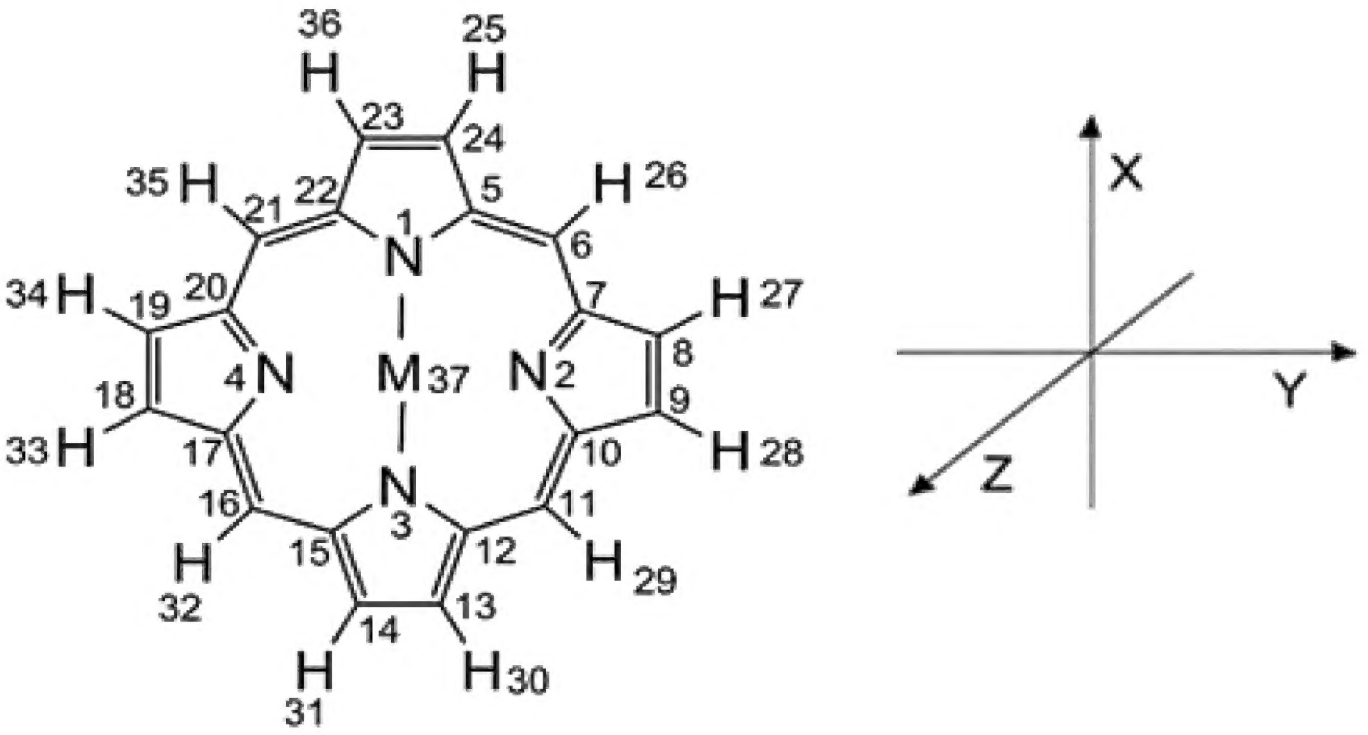

Figure 1. Structure of a metallporphine molecule with the system of numbering of the atoms followed throughout the discussion. M symbolizes any metal.

of dissociation, bond energy HOMO/LUMO energy level for single molecules were again computed using the single-point energy option key word.

Visualization of the HOMO/LUMO orbitals and changes of the electron density for particular molecules and their three molecule systems were performed involving the HyperChem 8.0 software (Froimowitz 1993).

Fig. 1 presents notation of particular atoms in metalloporphyrins.

Results and discussion

Based on the criterion of values of heat of formation (the stability of the system increases with declining negative value) (Table 1) the stability of metalloporphyrines under consideration declined in the order:

$$Fe(III)^{+} > Co(III)^{+} > Fe(II) > Co(II) > Cu(II) > Mg(II)$$

SMF destabilized the Mg(II)porphyrine. The value of heat formation gradually turned into less negative against an increase in applied flux density (Table 1). In every case the magnitude of the changes depended on the orientation of the molecule in the Cartesian system. The strongest destabilization was noted in the molecule oriented along the X-axis followed by its orientations along Y- and Z-axes, respectively. The changes in the heat of formation were accompanied by an increase in the values of dipole moment of the molecule. It rose depending in the same manner on the orientation of the molecule in the Cartesian system. Deformed porphyrin skeleton could take one of four conformations, that is, saddle (B_{2u}), ruffle (B_{1u}), dome (A_{2u}) or wave ($E_{gx,y}$) (Kingsbury and Senge 2021).

Table 1. Heat of formation [kJ.mol^{-1}] and dipole moment [D] of the metalloporphyrine molecules depending on applied SMF flux density [AMFU] and their situating in the Cartesian system.

SMF along indicated Cartesian axis	Heat of formation [kJ·mol^{-1}] at SMF flux density [AMFU]					Dipole moment [D] at SMF flux density [AMFU]				
	0	0.1	1.0	10	100	0	0.1	1.0	10	100
					Mg(II)					
X	-803	-781	-772	-731	-698	2.06	2.10	2.15	2.19	2.31
Z		-799	-794	-771	-726		2.09	2.10	2.11	2.18
Y		-796	-781	-762	-716		2.10	2.14	2.20	2.29
					Fe(II)					
X	-982	-972	-953	-911	-875	1.99	2.03	2.10	2.24	2.41
Z		-979	-967	-932	-904		2.01	2.06	2.11	2.24
Y		-979	-964	-936	-906		2.03	2.11	2.16	2.34
					Fe(III)+					
X	-1125	-1038	-987	-894	-815	2.06	2.11	2.19	2.35	2.62
Z		-1097	-1005	-974	-897		2.09	2.15	2.19	2.31
Y		-1023	-1000	-971	-902		2.11	2.24	2.32	2.62
					Co(II)					
X	-969	-942	-918	-781	-743	2.03	2.09	2.22	2.38	3.24
Z		-952	-947	-932	-918		2.06	2.15	2.21	2.38
Y		-946	-923	-761	-694		2.09	2.23	2.59	3.48
					Co(III)+					
X	-1021	-1014	-997	-876	-831	2.03	2.09	2.22	2.38	3.04
Z		-1006	-985	-934	-858		2.06	2.13	2.25	2.32
Y		-1015	-995	-968	-885		2.08	2.23	2.42	2.97
					Cu(II)					
X	-921	-892	-871	-811	-752	2.01	2.06	2.15	2.39	2.68
Z		-918	-906	-893	-812		2.03	2.06	2.09	1.98
Y		-885	-872	-803	-711		2.06	2.17	2.51	3.69

In Mg(II)porphyrine (Fig. 2), considered as very simplified model of chlorophyll, the central metal atom was not coordinated to the N2 and N4 ring nitrogen atoms. Planar structures (a) and (c) showed that one Mg-bound and one non-bound pyrrole rings were mostly responsible for the deformation of the molecule. Structures (b) revealed that the deformation led to bending of the molecule.

The shape of the porphyrin skeleton differed from the flat one characterized by the point group D_{4h}. It took the shape of a dome typical for the point group A_{2u}. The increase in SMF ejected the magnesium atom from the center of the molecule because of increasing lengths of the Mg-N bonds.

Corresponding variations of the charge density on the N- and Mg(II) atoms and the Mg(II)-N bond lengths are reported in Tables 2 and 3, respectively.

Data in Table 2 indicate irregular changes of the charge density at the N1 and N3 magnesium-bound atoms. Independently of the situating of the molecule against SMF, the charge at the N1 atom always remained negative. However, the charge density at the N3 magnesium bound atom situated along the Z-axis turned positive and also changed irregularly against applied flux density. The central Mg atom invariantly hold the positive charge density which irregularly rose with an increase in the flux density.

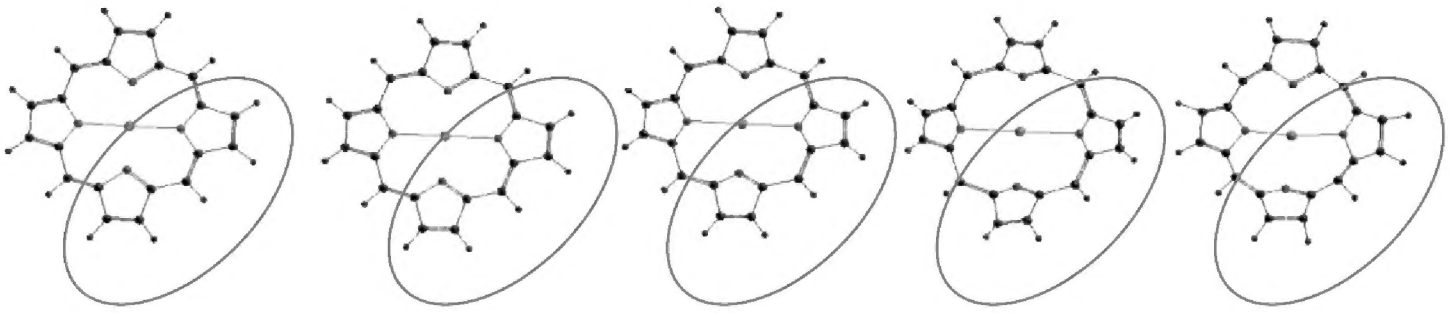

a

b

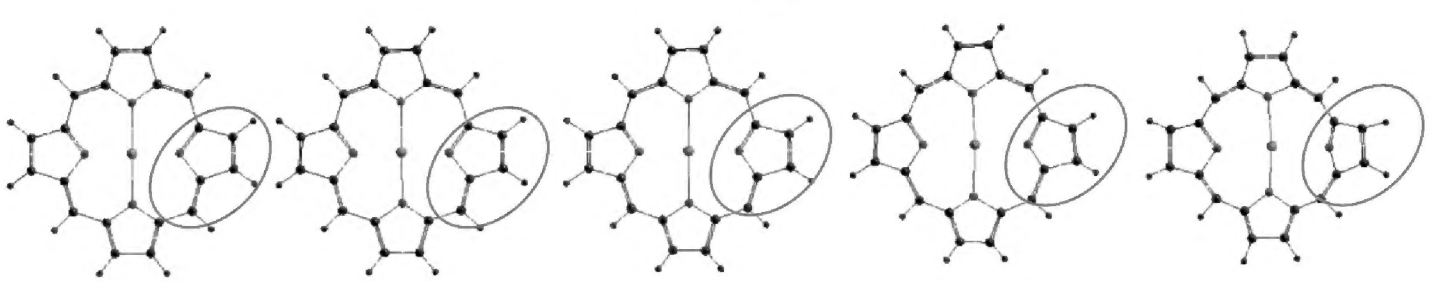

c

Figure 2. Deformation of Mg(II) porphyrine in SMF of 0 – 100 AMFU when the SMF direction is in (**a–c**) along X, Z and Y axes, respectively.

The smallest changes were noted in the molecule oriented along the Z-axis. Increasing charge density at the Mg atom should be beneficial for bonding Lewis bases. That is, it should promote photosynthesis provided the reaction site is not obscured by steric hindrances.

In their character the Mg-N bonds were intermediate between ionic and atomic, making the binding electron pair essential. Under the influence of a high external SMF, the durability of such a pair, maintained by magnetic forces, decreased. Thus, the bond become weaker and longer (Table 3).

Table 2. Charge density [a.u] at particular atoms of the Mg(II)porphyrine molecule depending on SMF flux density [AMFU] situating in the Cartesian system.

Atom	SMF along indicated Cartesian axis	Charge density [a.u] at SMF flux density [AMFU]				
		0	0.1	1.0	10	100
N1	X	-0.219	-0.095	-0.045	-0.297	-0.021
	Z		-0.212	-0.122	-0.118	-0.083
	Y		-0.067	-0.135	-0.249	-0.153
N3	X	-0.197	-0.192	-0.122	-0.255	-0.037
	Z		0.051	0.179	0.167	0.172
	Y		-0.167	-0.174	-0.218	-0.136
Mg37	X	0.387	0.637	0.638	0.538	0.532
	Z		0.521	0.546	0.556	0.577
	Y		0.626	0.640	0.567	0.646

Table 3. Bond lengths [Å] between particular atoms of the Mg(II)porphyrine molecule depending on SMF flux density [AMFU] situating in the Cartesian system.

Bond	SMF along indicated Cartesian axis	Bond length [Å] at flux density [AMFU]				
		0	0.1	1.0	10	100
N1-Mg37	X	1.917	2.161	2.286	2.125	2.438
	Z		2.111	2.045	2.077	2.156
	Y		2.096	2.140	2.066	2.136
N3-Mg37	X	1.898	2.169	2.298	1.944	2.459
	Z	2.109	2.061	2.090	2.126	
	Y	2.106	2.126	1.910	1.155	

The criterion of the heat of formation of Fe(II)porphyrine and Fe(III)porphyrine indicated that SMF destabilized these molecules.

The Fe(II) atom in Fe(II)porhyrine was tetracoordinated (Fig. 3).

Already out of SMF the molecule was non-planar and SMF considerably contributed to its deformation. In the molecule situated in the X-Y plane, particularly at 10 and 100 AMFU, remarkable charge density (Table 4) and elongation of some C-H bonds (Table 5) could be observed. The positive charge density at the Fe(II) atom slightly decreased with an increase in the applied flux density when the molecule was oriented along the X axis but, simultaneously increased in the molecules oriented along the Z and Y axes. Such response of the molecule to SMF was beneficial for the accepting Lewis bases, for instance, CO.

An elongation of the Fe-N was much less remarkable than that observed in Mg(II)porphyrine (Table 5). The mean value of the Fe-N bond length for all metalloporphyrines orientations along the SMF directions remained approximately constant. As with magnesium, electron density decreased on the atoms of nitrogen bound to iron, as well as on the iron itself, so the growing SMF caused the electrons to move to the periphery of the molecule.

The Fe(III) atom of Fe(III)porhyrine cation was also tetra-coordinated. Deformations of the molecules by increasing flux density are presented in Fig. 4.

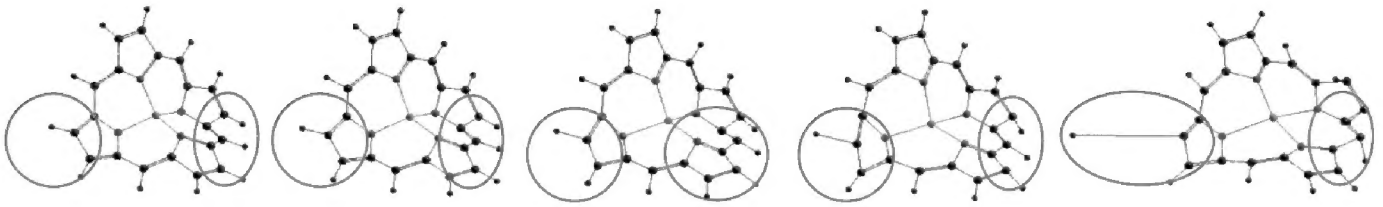

0 AMFU 0.1 AMFU 1.0 AMFU 10 AMFU 100 AMFU

a

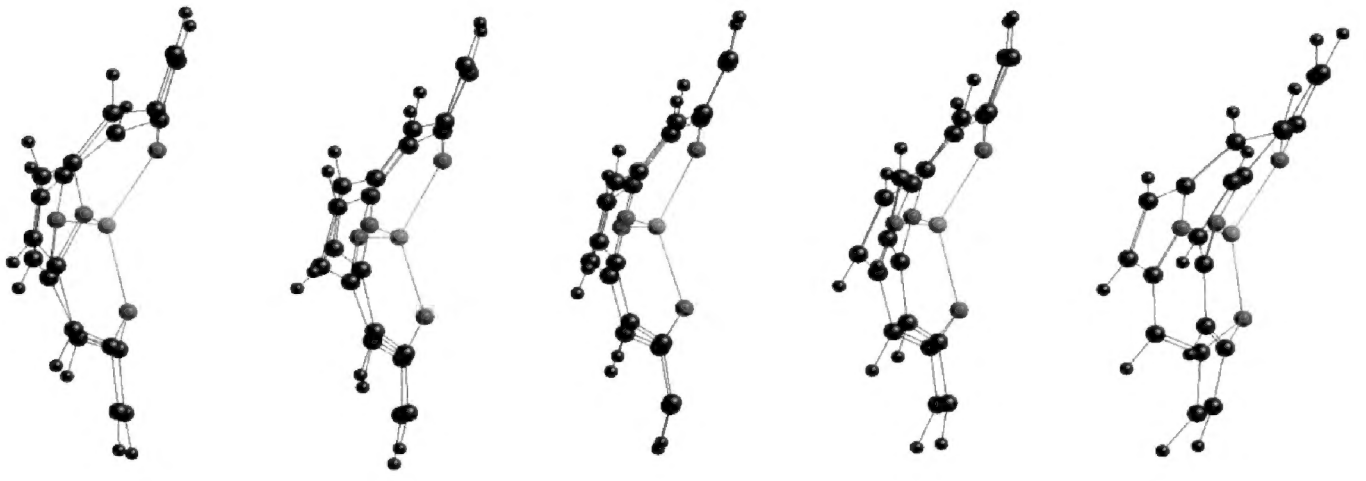

0 AMFU 0.1 AMFU 1.0 AMFU 10 AMFU 100 AMFU

b

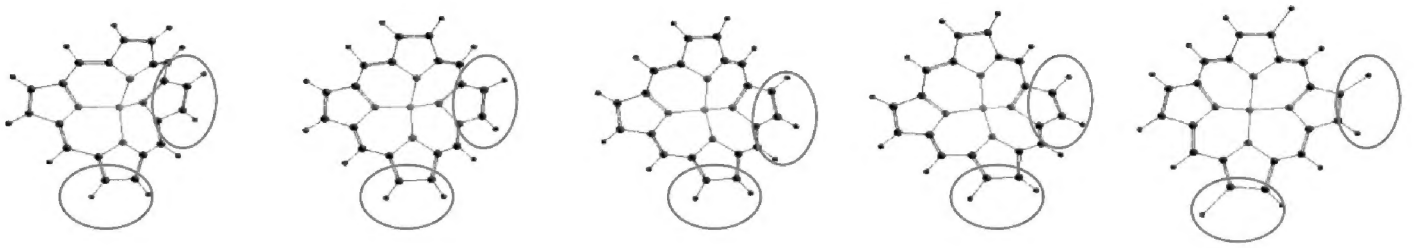

0 AMFU 0.1 AMFU 1.0 AMFU 10 AMFU 100 AMFU

c

Figure 3. Deformation of Fe(II)porphyrine in SMF of 0 – 100 AMFU when SMF direction is in (**a–c**) along X, Z and Y axes, respectively.

Table 4. Charge density [a.u.] at particular atoms of the Fe(II)porphyrine molecule depending on SMF flux density [AMFU] situating in the Cartesian system.

Atom	SMF along indicated Cartesian axis	Charge density [a.u] at SMF flux density [AMFU]				
		0	**0.1**	**1.0**	**10**	**100**
N1	X	-0.408	-0.379	-0.425	-0.252	-0.123
	Z		-0.384	-0.385	-0.375	0.004
	Y		-0.408	-0.425	-0.488	-0.439
N3	X	-0.346	-0.397	-0.315	-0.249	-0.199
	Z		-0.350	-0.325	-0.336	0.165
	Y		-0.501	-0.503	-0.438	-0.497
Fe37	X	1.651	1.602	1.473	1.212	1.039
	Z		1.734	1.685	1.661	1.019
	Y		1.845	1.823	1.822	1.769

Table 5. Bond lengths [Å] between particular atoms of the Fe(II)porphyrine molecule depending on SMF flux density [AMFU] situating in the Cartesian system.

Bond	SMF along indicated Cartesian axis	Bond length [Å] at flux density [AMFU]				
		0	0.1	1.0	10	100
N2-Fe37	X	1.893	1.994	2.170	2.047	2.109
	Z		1.730	1.794	1.770	1.787
	Y		1.782	1.658	1.763	1.801
N3-Fe37	X	1.898	1.926	2.170	2.214	2.644
	Z		1.855	1.840	1.860	1.885
	Y		1.689	1.692	1.738	1.772

Compared to Fe(II)porphirine the porphine skeleton localized along X and Z axes faced only slight deformation evoked by SMF.

Relevant charge density at particular atoms and bond lengths are collected in Tables 6 and 7, respectively.

An increase in applied SMF resulted in an irregular change of the positive charge density of the Fe atom. A general tendency in decrease of that charge was perturbed mainly in the molecules oriented against SMF along Z-axis. The same effect could be observed for negative charge density at the N1 and N3 atoms which, generally, decreased with an increase in applied SMF (Table 6). Thus, the flux density of 0.1 and 1.0 AMFU should facilitate reactions of the Fe(III) atom with Lewis bases.

Such irregularities were accompanied with irregular changes of the N-Fe bond lengths. These bonds generally were elongated with an increase in applied SMF (Table 7).

An insight in Table 1 showed that SMF destabilized Co(II) and Co(III)porphyrines and negatively influenced their biological functions.

The Co(II) atom in Co(II)porphyrine remained bidentate. Its presence inhibited to a great extent the deformation of the molecule involving bending molecule typical for formerly mentioned metalloporphyrines (Fig. 5). Instead, a local deformation within the macrocyclic took place. Corresponding charge density and bond lengths computed for these molecule are presented in Tables 12 and 13, respectively.

The SMF acting along the Z- axis flatted the molecule. The increase in SMF changed the conformations in the order: dome-flat-flat-dome with simultaneous distancing of the cobalt atom from the plane of the molecule.

The action of SMF along the X or Y axis evoked a wave mode deformation, with a point group $E_{gx,y}$ (Kingsbury and Senge 2021).

The applied SMF atom always affected the negative charge density at the N-atoms and positive charge density at the Co-atom. These changes were chimerically dependent on the orientation of the molecules against SMF (Table 8). However, always resulting charge density at the Co(II) atom increased in respect to that in the molecule out of SMF. Thus, the ability of the Co(II) atom to bind Lewis bases increased. Molecules oriented against SMF along the Y axis should react with Lewis bases the most readily.

The SMF also influenced and extended the length of both N-Co bonds and that effect was strongly dependent on the orientation of the molecule against the SMF (Table 9).

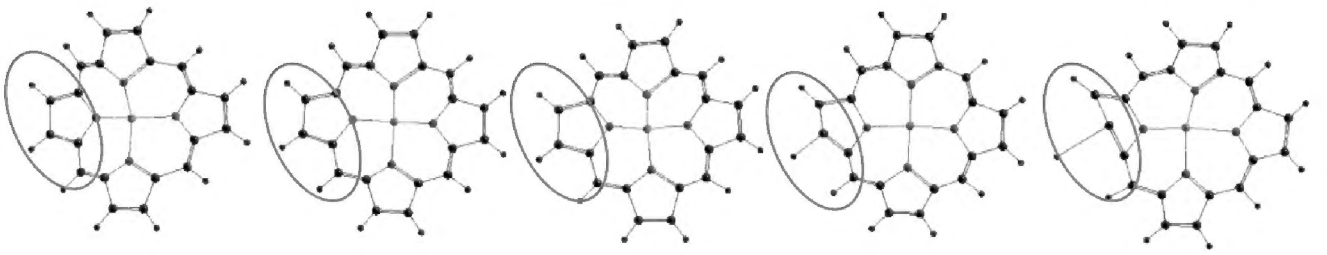

0 AMFU 0.1 AMFU 1.0 AMFU 10 AMFU 100 AMFU

a

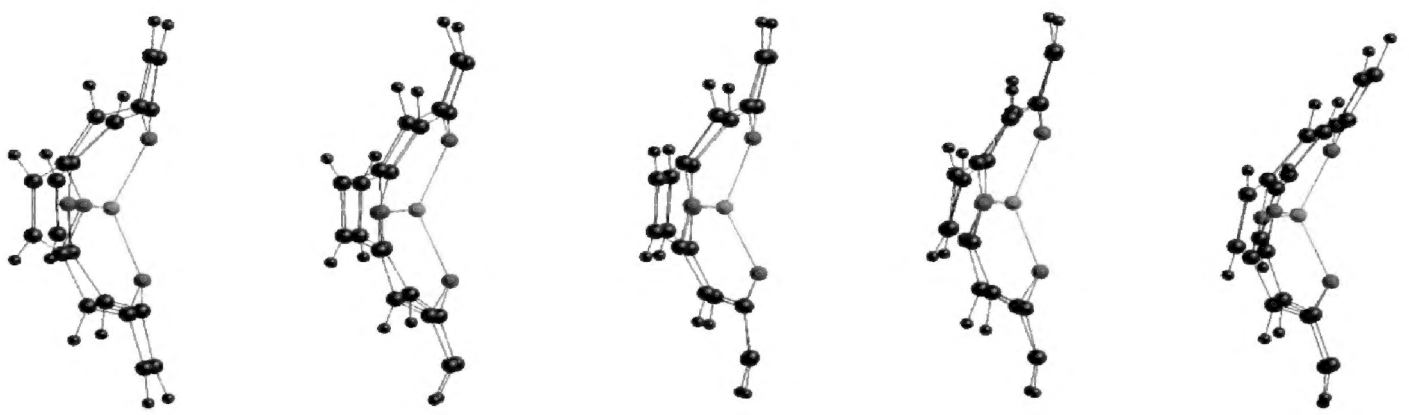

0 AMFU 0.1 AMFU 1.0 AMFU 10 AMFU 100 AMFU

b

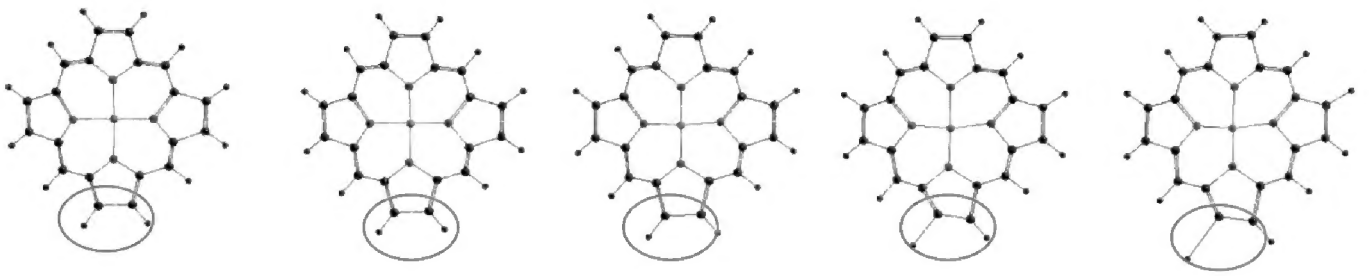

0 AMFU 0.1 AMFU 1.0 AMFU 10 AMFU 100 AMFU

c

Figure 4. Deformation of Fe(III)porphyrine in SMF of 0 – 100 AMFU when the SMF direction is in (**a–c**) along X, Z and Y axes, respectively.

The Co(III) atom in Co(III)porphyrine cation also remained bidentate and, principally, it also inhibited deformation of the molecule by bending. In comparison to Co(II) atom its presence in the macrocyclic ring favoured elongation of some C-H bonds to the extent suggesting their dissociation (Fig. 6).

The action of the SMF along each axis causes deformation of the flat system to corrugated, wave mode $E_{gx,y}$ (Kingsbury and Senge 2021).

The relevant changes of the charge density at Co and N atoms and the Co-N atom bonds are reported in Tables 10 and 11, respectively. As in the case of formerly presented

Table 6. Charge density [a.u.] at particular atoms of the Fe(III)porphyrine molecule cation depending on SMF flux density [AMFU] situating in the Cartesian system.

Atom	SMF along indicated Cartesian axis	Charge density [a.u] at SMF flux density [AMFU]				
		0	0.1	1.0	10	100
N1	X	-0.354	-0.457	-0.465	-0.437	-0.065
	Z		-0.430	-0.382	-0.403	-0.423
	Y		-0.455	-0.452	-0.057	-0.082
N3	X	-0.363	-0.400	-0.395	-0.329	-0.073
	Z		-0.352	-0.385	-0.396	-0.414
	Y		-0.451	-0.441	-0.149	-0.121
Fe37	X	1.696	1.767	1.765	1.429	0.928
	Z		1.654	1.726	1.765	1.807
	Y		1.787	1.797	1.154	1.199

Table 7. Bond lengths [Å] between particular atoms of the Fe(III)porphyrine molecule cation depending on SMF flux density [AMFU] situating in the Cartesian system.

Bond	SMF along indicated Cartesian axis	Bond length [Å] at flux density [AMFU				
		0	0.1	1.0	10	100
N1-Fe37	X	1.917	1.802	1.820	1.997	2.173
	Z		1.905	1.828	1.886	1.803
	Y		1.822	1.835	1.912	1.945
N3-Fe37	X	1.873	1.823	1.809	2.140	2.126
	Z	1.950	1.807	1.796	1.723	
	Y	1.897	1.798	1.863	1.835	

metalloporphyrines, these changes with an increase in applied flux density were irregular and strongly dependent on the orientation of the molecules against SMF. In contrast to Co(II)porphyrine where SMF facilitated reaction of the central metal atom with Lewis bases, SMF flux density decreased the ability of the Co(III) to bind Lewis bases.

SMF negatively perturbs biological functions of Cu(II)porphyrine as it increased its heat of formation (Table 1).

Inserting the Cu(II) atom into the porphine ring produced its deformation by bending already out of SMF.

An increase in SMF caused a change in conformation from the dome to the flat one. It distinguished Cu(II)porphyrine from those discussed above. The presence of the Cu(II) atom favored considerable elongation of the C-H bonds.

Charge density distribution in this molecule and relevant bond lengths are grouped in Tables 12 and 13, respectively.

Performed computations presented fairly unusual effects of insertion of Cu(II) atom into porphine. Thus, already in the molecule out of SMF both nitrogen atoms bound to the Cu(II) atom hold the positive charge density. Already SMF of flux density of 0.1 AMFU turned the charge density at the N1 atom into negative when the molecule was oriented along either X or Z axis. In the molecule oriented along the Y axis just the flux density of 100 AMFU developed negative charge density at that atom.

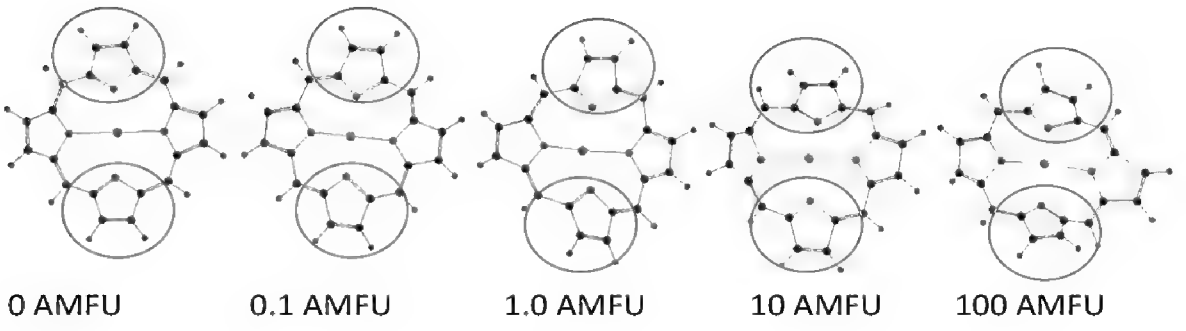

a

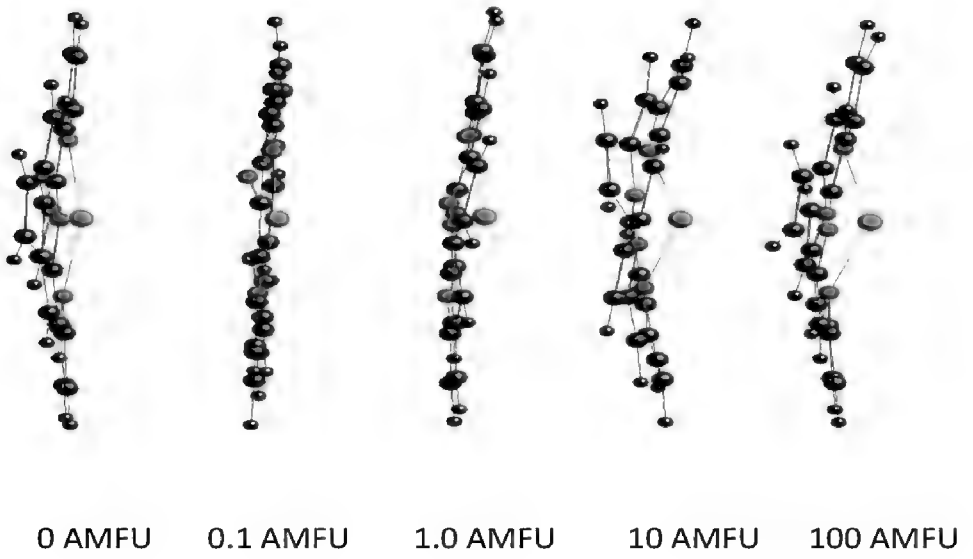

b

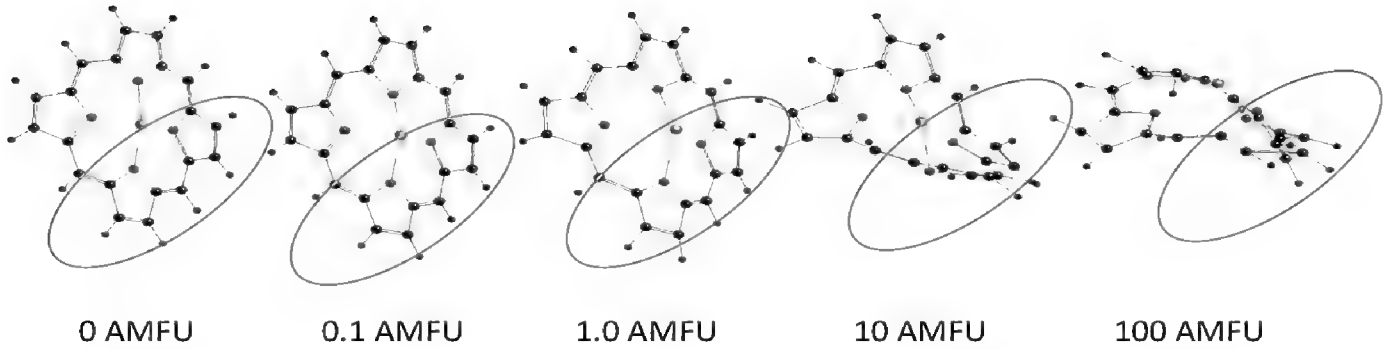

c

Figure 5. Deformation of Co(II) porphyrine in SMF of 0 – 100 AMFU when the SMF direction is in (**a–c**) along X, Z and Y axes, respectively.

Table 8. Charge density [a.u] at particular atoms of the Co(II)porphyrine molecule depending on SMF flux density [AMFU] situating in the Cartesian system.

Atom	SMF along indicated Cartesian axis	Charge density [a.u] at SMF flux density [AMFU]				
		0	0.1	1.0	10	100
N1	X	-0.218	-0.094	-0.247	-0.149	-0.059
	Z		-0.226	-0.118	-0.144	0.085
	Y		-0.214	-0.281	-0.190	-0.129
N3	X	-0.220	-0.149	-0.164	-0.259	-0.288
	Z		-0.034	-0.160	-0.126	-0.227
	Y		-0.201	-0.254	-0.094	0.131
Co37	X	0.509	0.584	0.705	0.611	0.878
	Z		0.587	0.596	0.574	0.467
	Y		0.605	0.754	0.596	0.971

Table 9. Bond lengths [Å] between particular atoms of the Co(II)porphyrine molecule depending on SMF flux density [AMFU] situating in the Cartesian system.

Bond	SMF along indicated Cartesian axis	Bond length [Å] at flux density [AMFU]				
		0	0.1	1.0	10	100
N1-Co37	X	1.958	2.054	2.138	2.224	2.202
	Z		2.011	2.064	1.889	1.925
	Y		2.113	2.323	2.450	2.406
N3-Co37	X	1.945	2.036	2.123	2.142	2.394
	Z		2.139	2.052	1.090	1.892
	Y		1.862	2.230	1.926	2.745

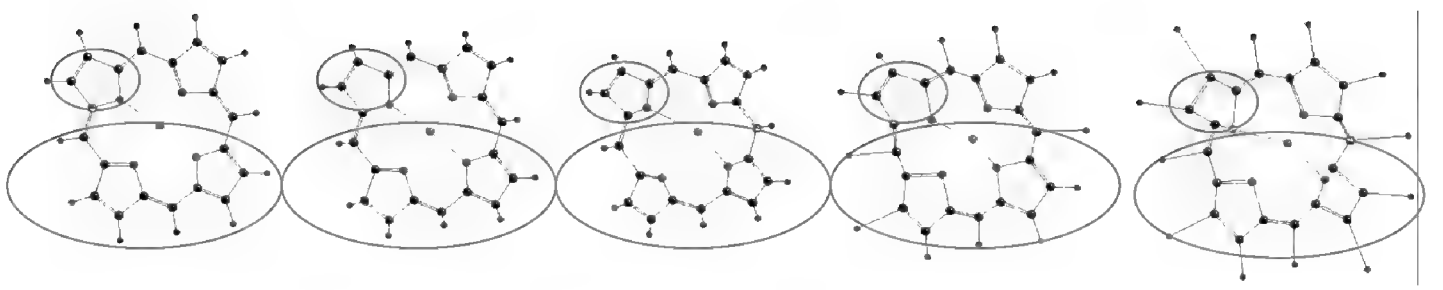

a

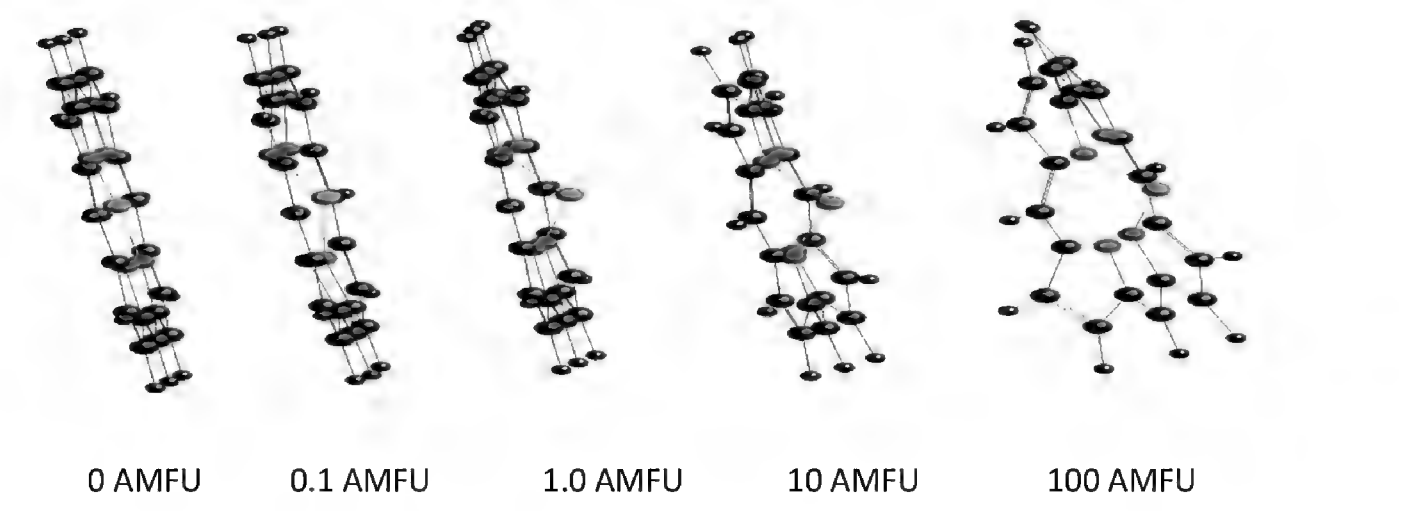

b

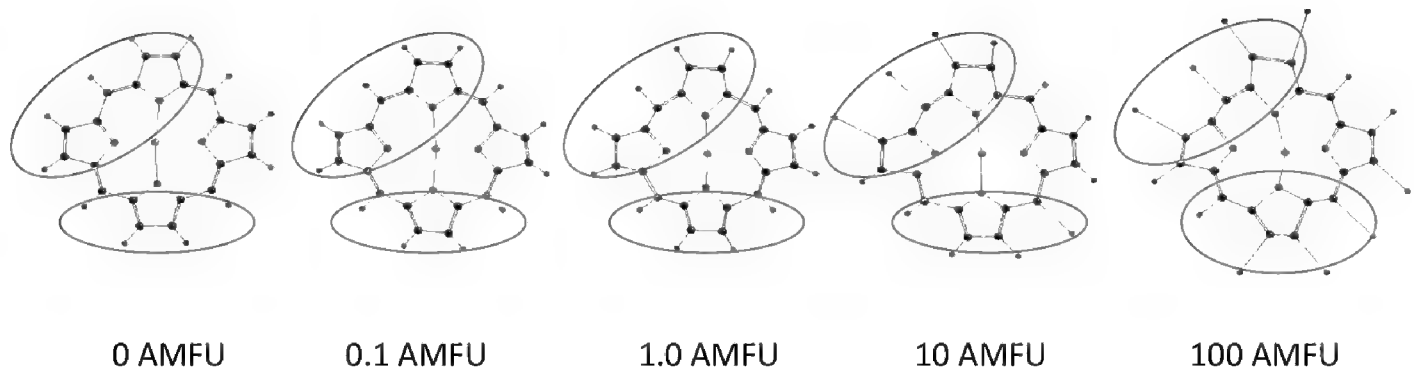

c

Figure 6. Deformation of Co(III)porphyrine in SMF of 0 – 100 AMFU when the SMF direction is in (**a–c**) along X, Z and Y axes, respectively.

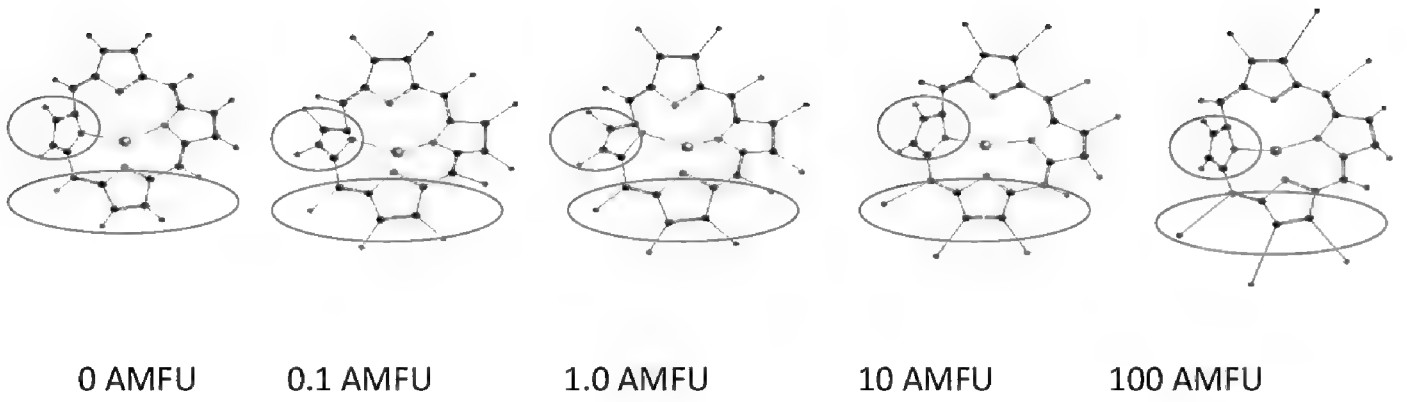

a

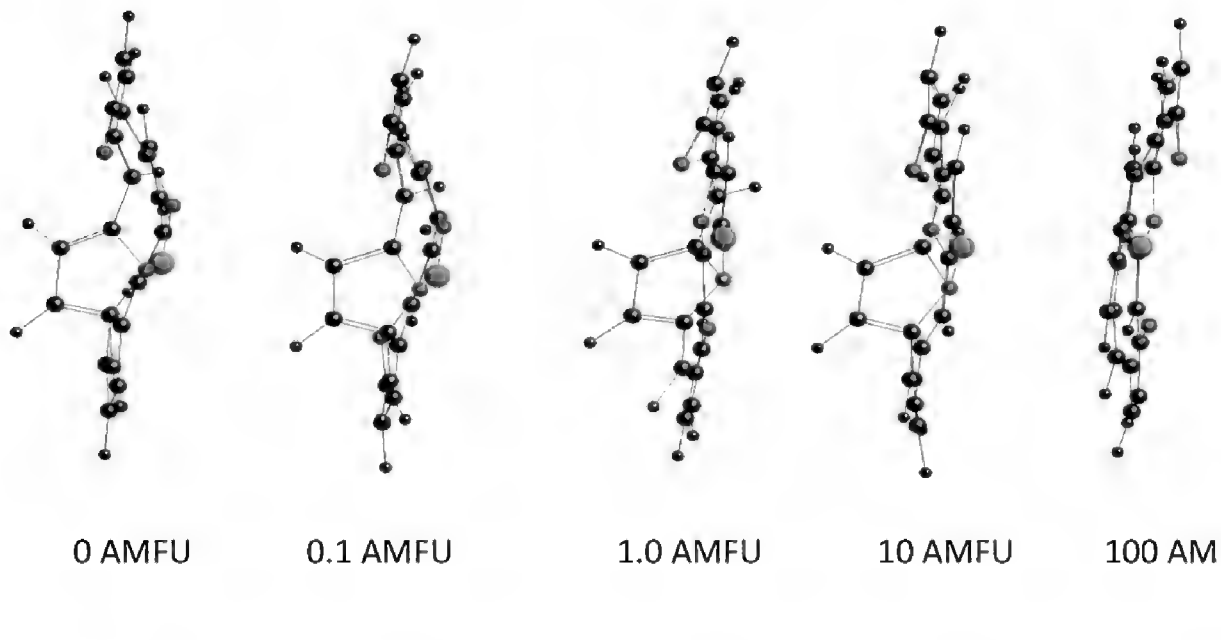

c

Figure 7. Deformation of Cu(II)porphyrine in SMF of 0 – 100 AMFU when the SMF direction is in (**a–c**) along X, Z and Y axes, respectively.

The N3 atom appeared to be more susceptible to the conversion of its initial positive charge density into negative. In the molecule located along the X axis solely flux density of 0.1 AMFU could not convert that charge density into negative. In all remained cases the charge density at that atom readily converted into negative.

Applied SMF invariantly increased positive charge density at the Cu atom (Table 12) what should facilitate coordination of Lewis bases. The length of both N-Cu bonds varied irregularly with an increase in the applied flux density and orientation against

Table 10. Charge density [a.u] at particular atoms of the Co(III)porphyrine molecule cation depending on SMF flux density [AMFU] situating in the Cartesian system.

Atom	SMF along indicated Cartesian axis	Charge density [a.u] at SMF flux density [AMFU]				
		0	0.1	1.0	10	100
N1	X	-0.243	-0.205	-0.048	-0.052	-0.017
	Z		-0.223	-0.200	-0.200	0.034
	Y		-0.303	-0.378	-0.303	-0.252
N3	X	-0.304	-0.270	-0.004	-0.365	0.516
	Z		-0.258	-0.161	-0.147	0.134
	Y		-0.358	-0.312	-0.186	-0.337
Co37	X	1.223	1.247	1.220	1.018	0.651
	Z		1.158	1.175	1.155	0.864
	Y		1.206	1.110	1.188	0.946

Table 11. Bond lengths [Å] between particular atoms of the Co(III)porphyrine molecule cation depending on SMF flux density [AMFU] situating in the Cartesian system.

Bond	SMF along indicated Cartesian axis	Bond length [Å] at flux density [AMFU]				
		0	0.1	1.0	10	100
N1-Co37	X	2.052	2.181	2.471	1.979	2.497
	Z		2.053	1.899	1.859	1.867
	Y		2.049	1.892	1.967	1.930
N3-Co37	X	2.064	2.069	1.972	1.588	2.221
	Z		2.106	1.910	1.921	1.956
	Y		2.027	1.646	1.961	1.779

Table 12. Charge density [a.u] at particular atoms of the Cu(II)porphyrine molecule depending on SMF flux density [T] situating in the Cartesian system.

Atom	SMF along indicated Cartesian axis	Charge density [a.u] at SMF flux density [AMFU]				
		0	0.1	1.0	10	100
N1	X	0.202	-0.237	-0.259	-0.534	-0.473
	Z		-0.235	-0.260	-0.248	-0.202
	Y		0.109	0.054	0.012	-0.241
N3	X	0.040	0.061	-0.227	-0.465	-0.413
	Z		-0.137	-0.258	-0.165	-0.124
	Y		-0.160	-0.084	-0.120	-0.302
Cu37	X	0.726	0.907	0.814	0.962	0.942
	Z		0.967	1.003	1.076	0.911
	Y		0.847	0.790	0.882	0.993

SMF. The N-Cu bonds were the least sensitive to elongation when the molecule was oriented along the Z- axis (Table 13).

Thus, in summary, static magnetic field (SMF) decreased stability of the metalloporphyrine molecules. This effect depended on the situating of the molecule in respect to the direction of SMF of the Cartesian system. An increase in the value of heat

Table 13. Bond lengths [Å] between particular atoms of the Cu(II)porphyrine molecule depending on SMF flux density [AMFU] situating in the Cartesian system.

Bond	SMF along indicated Cartesian axis	Bond length [Å] at flux density [AMFU]				
		0	0.1	1.0	10	100
N1-Cu37	X	1.964	1.649	1.437	2.046	1.991
	Z		1.962	1.975	2.058	1.947
	Y		2.213	1.932	2.243	2.884
N3-Cu37	X	1.966	2.166	2.172	1.836	1.860
	Z		1.956	1.961	2.045	2.032
	Y		2.044	2.060	2.132	2.483

of formation was accompanied by an increase in dipole moment. It was an effect of deformations of the molecule which involved pyrrole rings holding the hydrogen atoms at the ring nitrogen atoms and the length of the C-H and N-H bonds. As a consequence that macrocyclic ring lost its planarity. Recently, (Kong et al. 2022) discovered in the Milky Way the Highest-energy CRSF from the First Galactic Ultraluminous X-Ray Pulsar Swift J0243.6+6124. It reached over 1.6 billion Tesla. The presence of multipole field components close to the surface of the neutron star confirms deteriorating effect of SMF of high density upon metalloporphyrines suggested by performed in silico computations described in this paper.

Conclusions

SMF even of the lowest, 0.1 AMFU flux density influences the biological role of metalloporphyrines associated with their central metal atoms. This effect is generated by changes in the electron density at these atoms, its steric hindering and polarization of particular bonds from pure valence bonds possibly into ionic bonds. Regardless of its situation along x, y and z axis, SMF always destabilized the metalloporphyrine molecules. Evoked deformation of particular molecules facilitated additional ligation of the central metal atom. Potentially, this effect could be used in synthetic modifications of metalloporphyrines.

References

Anderson S, Anderson HL, Bashall A, McPartlin M, Sanders JKM (1995) Assembly and crystal structure of a photoactive array of five porphyrins. Angewandte Chemie 34(10): 1096–1099. https://doi.org/10.1002/anie.199510961

Carpenter JE, Weinhold F (1988) Analysis of the geometry of the hydroxymethyl radical by the different hybrids for different spins natural bond orbital procedure Journal of Molecular Structure (Teochem) 139: 41–62. https://doi.org/10.1016/0166-1280(88)80248-3

Charistos ND, Munoz-Castro A (2019) Double aromaticity of the B-40 fullerene: Induced magnetic field analysis of pi and sigma delocalization in the boron cavernous structure.

Physical Chemistry Chemical Physics 21(36): 20232–20238. https://doi.org/10.1039/C9CP04223G

Ciesielski W, Girek T, Oszczęda Z, Soroka JA, Tomasik P (2022) Potential risk resulting from the influence of static magnetic field upon living organisms. Numerically simulated effects of the static magnetic field upon porphine. BioRisk 18: 93–104. https://doi.org/10.3897/biorisk.18.80607

Farberovich OV, Mazalova VL (2016) Ultrafast quantum spin-state switching in the Co-octaethylporphyrin molecular magnet with a terahertz pulsed magnetic field. Journal of Magnetism and Magnetic Materials 405: 169–173. https://doi.org/10.1016/j.jmmm.2015.12.038

Frisch MJ, Trucks GW, Schlegel HB, Scuseria GE, Robb MA, Cheeseman JR, Scalmani G, Barone V, Mennucci B, Petersson GA (2016) Gaussian 09, Revision A.02, Gaussian, Inc., Wallingford CT.

Froimowitz M (1993) HyperChem: A software package for computational chemistry and molecular modelling. BioTechniques 14: 1010–1013.

Glendening ED, Reed AE, Carpenter JE, Weinhold F (1987) Extension of Lewis structure concepts to open-shell and excited-state molecular species, NBO Version 3.1, PhD thesis, University of Wisconsin, Madison, WI.

Hodak E, Pavlovsky L (2015) Phototherapy of mycosis fungoides. Dermatologic Clinics 33(4): 697–702. https://doi.org/10.1016/j.det.2015.05.005

Huang H, Song W, Rieffel J, Lovell JF (2015) Emerging applications of porphyrins in photomedicine. Frontiers in Physics 3: e23. [1–15] https://doi.org/10.3389/fphy.2015.00023

Kadish KM, Smith KM, Guilard R [Eds] (2000) Porphyrin Handbook. Academic Press, San Diego.

Kingsbury JC, Senge MO (2021) The shape of porphyrins. Coordination Chemistry Reviews 431: 213760. https://doi.org/10.1016/j.ccr.2020.213760

Kong L-D, Zhang S, Zhang S-N, Ji L, Doroshenko V, Santangelo A, Chen Y-P, Lu F-J, Ge M-Y, Wang P-J, Tao L, Qu J-L, Li T-P, Liu C-Z, Liao J-Y, Chang Z, Peng J-Q, Shui Q-C (2022) Insight-HXMT discovery of the highest-energy CRSF from the first galactic ultra-luminous X-ray pulsar swift J0243.6+6124. The Astrophysical Journal. Letters 933(1): L3. https://doi.org/10.3847/2041-8213/ac7711

Marchand N, Lienard P, Siehl H, Harunobu I (2014) Applications of molecular simulation software SCIGRESS in industry and university. Fujitsu Scientific and Technical Journal 50(3): 46–51.

Ortiz de Montellano PR (2008) Hemes in Biology. Wiley Encyclopedia of Chemical Biology. John Wiley & Sons. https://doi.org/10.1002/9780470048672.wecb221.

Ptaszek M (2013) Rational design in fluorophores for *in vitro* applications. In: Morris MC (Ed.) Progress in Molecular Biology and Translational Science, vol. 113 Fluorescence – based Biosensors, from Concepts to Applications, Fluorescence-Based Biosensors in Progress in Molecular Biology and Translational Science. Academic Press, Oxford. https://doi.org/10.1016/B978-0-12-386932-6.00003-X

Scheidt WR, Lee YJ (1987) Recent advances in the stereochemistry of metallotetrapyrroles. In: Buchler JW (Ed.) Metal Complexes with Tetrapyrrole Ligands I. Structure and Bonding, vol 64. Springer, Berlin, Heidelberg. https://doi.org/10.1007/BFb0036789.

Stevens JM, Daltrop O, Allen JWA, Fergusson SJ (2004) C-type cytochrome formation: Chemical and biological enigmas. Accounts of Chemical Research 37(12): 999–1007. https://doi.org/10.1021/ar030266l

Walter MG, Rudine AB, Wamser CC (2010) Porphyrins and phthalocyanines in solar photovoltaic cells. Journal of Porphyrins and Phthalocyanines 14(09): 759–792. https://doi.org/10.1142/S1088424610002689

Yella A, Lee HW, Tsao HN, Yi C, Chandiran AK, Nazeeruddin MK, Diau EW-G, Yeh C-Y, Zakeeruddin SM, Grätzel M (2011) Chandiran AK, Nazeeruddin K et al. Porphyrin-sensitized solar cells with cobalt (II/III)–based redox electrolyte exceed 12 percent efficiency. Science 334(6056): 629–634. https://doi.org/10.1126/science.1209688